An experimental validation of a turbulence model for air flow in a mining chamber

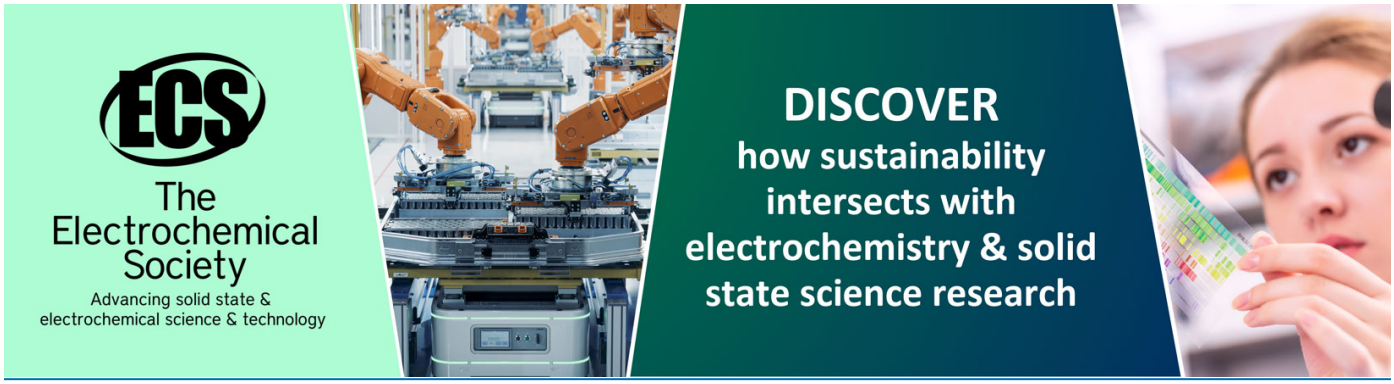

An Experimental Validation of a Turbulence Model for Air Flow in a Mining Chamber

M. Branny[1*], M. Karch[1], W. Wodziak[1], M. Jaszczur[2], R. Nowak[2], J.S. Szmyd[2]
[1]Faculty of Mining and Geoengineering
[2]Faculty of Energy and Fuels
AGH University of Science and Technology, Krakow, Poland

e-mail: branny@agh.edu.pl

Abstract. In copper mines, excavation chambers are ventilated by jet fans. A fan is installed at the inlet of the dead-end chamber, which is usually 20-30m long. The effectiveness of ventilation depends on the stream range generated by the fan. The velocity field generated by the supply air stream is fully three-dimensional and the flow is turbulent. Currently, the parameters of 3D air flows are determined using the CFD approach. This paper presents the results of experimental testing and numerical simulations of airflow in a laboratory model of a blind channel, aired by a forced ventilation system. The aim of the investigation is qualitative and quantitative verification of computer modelling data. The analysed layout is a geometrically re-scaled and simplified model of a real object. The geometrical scale of the physical model is 1:10. The model walls are smooth, the channel cross-section is rectangular. Measurements were performed for the average airflow velocity in the inlet duct equal 35.4m/s, which gives a Reynolds number of about 180 000. The components of the velocity vector were measured using the Particle Image Velocimetry approach. The numerical procedures presented in this paper use two turbulence models: the standard k-ε model and the Reynolds Stress model. The experimental results have been compared against the results of numerical simulations. In the investigated domain of flow - extending from the air inlet to the blind wall of the chamber - we can distinguish two zones with recirculating flows. The first, reaching a distance of about 1m from the inlet is characterized by intense mixing of air. A second vortex is formed into a distance greater than 1m from the inlet. Such an image of the velocity field results from both the measurements and calculations. Based on this study, we can conclude that the RSM model provides better predictions than the standard k-ε model. Good qualitative agreement is achieved between Reynolds Stress model predictions and measured components of the velocity.

1. Introduction

Mine headings in board and pillar excavation system are typically ventilated with the use of jet fans. Polish copper mining widely used such ventilation systems. Most headings are 20-30m long and fans are typically installed at the inlet to the heading. The ventilation efficiency depends on the range of air jet generated by the fan. The air jet penetration distance is influenced by a number of factors, among them such as inlet air flow rate, the flow velocity or the intensity of turbulence. In real flow the velocity field generated by the supply air stream is fully three-dimensional and the flow is unsteady and fully turbulent. Currently the parameters of 3D air flows are determined using the CFD (Computational Fluid Dynamics) approach [1]-[5]. The validation test of CFD simulation results for

the air flow in the mining face area was done in [7]-[10]. The flow field, investigated in this paper differs significantly from those analyzed in the mentioned papers where the connections between the ventilation ducts has been arranged different way.

This paper presents the result of experimental and numerical predictions of airflow in a laboratory model of a blind heading ventilated by a jet fan. The heading geometry considered in the study is a re-scaled and simplified in reference to the real object. The walls of the model representing chamber and main gallery are smooth and the channels cross-sections are rectangular. The fan generating the air jet is located beyond the measurement section. The measurements were performed for the steady and isothermal flow conditions. In that case, an equal Reynolds number in the model and in the real object assures that the flow criteria are similar. Air was used as the experimental fluid in the laboratory stand, thus the equality of the Prandtl number was fulfilled.

The components of the velocity vector were measured using the Particle Image Velocimetry (PIV) approach. The numerical procedures presented in this paper use two turbulence models: the standard k-ε model and the Reynolds Stress Model (RSM). Numerical calculations are supported by the Ansys Fluent software . The main objective of this research is the qualitative and quantitative verification of modelling results.

2. Experimental set-up

Experimental measurements were conducted in a laboratory settings (shown schematically in Fig.1), incorporating two intersecting rectangular channels with a cross-section of 0.4 x 0.2 m. The blind chamber is 3.35 m length. Air is supplied with a 3.0 m long tube , where the tube diameter is 0.076 m. Measurement is done on a purpose-built 1:10 scale model of the real object. In order to obtain the axisymmetric flow velocity profile at the inlet to the chamber a 1.35 m jet-stabilised section was provided to stabilise the air jet. The stabiliser comprises a diffuser, a confuser and a 0.2 m diameter tube. The distance between the axis of the air-supply duct to the upper and side walls of the blind chamber is 0.08 m. The air inlet is at the distance of 2.0 m from the chamber's blind wall, which is a typical chamber length in copper mines, re-scaled accordingly.

The measuring PIV system was subjected to testing and calibration procedures under flow condition to yield the number of registered flow images required to ensure accurate statistics (around 1000) and the size of the optimal interrogation window for the cross-correlation method (32x32 pixels). The Davis software was used to analyse the images to evaluate the velocity vector components.

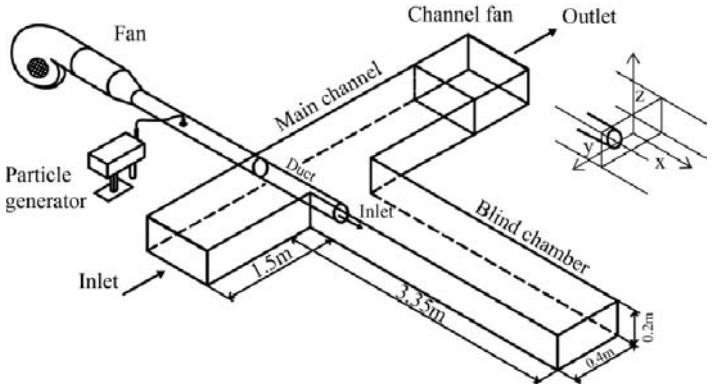

Figure 1. Schematic diagram of the measurement set-up.

3. Mathematical model

Classical modeling of turbulence is based on the Reynolds concept, which for incompressible and Newtonian fluids yields the following equations [6]

$$\frac{\partial U_i}{\partial x_i} = 0 \tag{1}$$

$$\frac{\partial U_i}{\partial t} + U_j \frac{\partial U_i}{\partial x_j} = -\frac{1}{\rho}\frac{\partial P}{\partial x_i} + \frac{\partial}{\partial x_j}\left(\nu \frac{\partial U_i}{\partial x_j} - \overline{u_i u_j}\right) \tag{2}$$

$$-\overline{u_i u_j} = \nu_t \left(\frac{\partial U_i}{\partial x_j} + \frac{\partial U_j}{\partial x_i}\right) - \frac{2}{3}\rho k \delta_{ij} \tag{3}$$

where: $\nu_t = C_\mu \frac{k^2}{\varepsilon}$ is the turbulent viscosity, k is kinetic energy, ε is the dissipation rate of k, C_μ is the constant, δ_{ij} the Kronecker delta, U_i and u_i the mean and fluctuating components of velocity, ρ the density, P the pressure, and ν the molecular viscosity.

In this study, two models of turbulence were tested: the standard k-ε model and the Reynolds stress model. The standard k-ε model is the most widely used turbulent model for solving industrial problems, particularly in mining for solving ventilation problems. This is a semi-empirical model based on the Boussinesq's conception of turbulent viscosity and on two transport equations for turbulent kinetic energy and its dissipation rate (equations (4) and (5)).

$$\frac{\partial k}{\partial t} + U_i \frac{\partial k}{\partial x_i} = \frac{\partial}{\partial x_i}\left(\left(\nu + \frac{\nu_t}{\sigma_k}\right)\frac{\partial k}{\partial x_i}\right) - \overline{u_i u_j}\frac{\partial U_i}{\partial x_j} - \varepsilon \tag{4}$$

$$\frac{\partial \varepsilon}{\partial t} + U_i \frac{\partial \varepsilon}{\partial x_i} = \frac{\partial}{\partial x_i}\left(\left(\nu + \frac{\nu_t}{\sigma_\varepsilon}\right)\frac{\partial \varepsilon}{\partial x_i}\right) - C_1 \frac{\varepsilon}{k}\overline{u_i u_j}\frac{\partial U_i}{\partial x_j} - C_2 \frac{\varepsilon^2}{k} \tag{5}$$

where C_1, C_2, σ_k, σ_ε are constants [6].

The Reynolds Stress Model (RSM) closes two systems of equations (1), (2) by solving transport equations for Reynolds stresses, together with an equation for the dissipation rate. The RSM is expected to give most accurate predictions for complex turbulent flows. A wall function was used in the near-wall region.

3.1. Mesh size

A structured, non-uniform mesh was generated for the computational domain. Three different size meshes of about 1,200,000, 2,800,000 and 5,600,000 cells were examined. The most visible effects of mesh refinement may be observed in cross-sections further apart from the inlet opening, especially in lower chamber region and the results for two finer meshes differ slightly in comparison with the coarse one. Thus, the mesh consisting of 5,600,000 cells was used in further calculations.

4. Numerical procedure

In the numerical procedure, the boundary conditions at the inlet were expressed by the experimental velocity profile of the air jet entering the test section in the laboratory model (see Fig 2).

The mean velocity at the inlet to the blind chamber was U=35,4m/s and the corresponding Reynolds number was approximately Re=180 000.

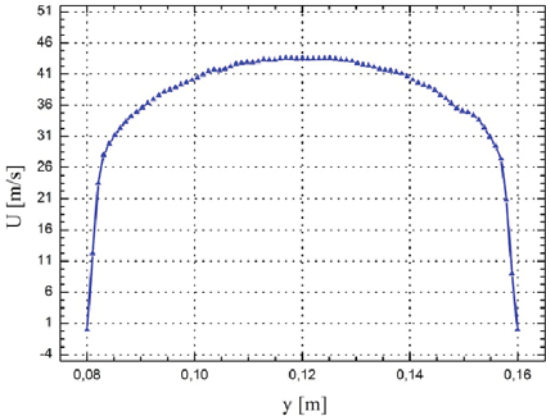

Figure 2. Velocity profile at the inlet to the blind chamber.

The kinetic energy of turbulence, based on the velocity fluctuation measured in the axis of the inlet, was equal to 5.9m^2/s^2. The calculated turbulence intensity was 5.6% while the length scale was 0,00532m.

The velocity field in the inlet cross-section of the main duct was assumed to be uniform. Measured average velocity was 2,1m/s, the intensity of turbulence 5% and the length scale 0.0187 m.

Boundary conditions on walls were assumed in the form of wall functions. The distance between the nodes nearest to the walls should be such that it would fall in the lower range of validity of the logarithmic law for mean velocity. In the calculation procedure this distance was controlled by the parameter y^* :

$$y^* = \frac{\rho C^{1/4} k_P^{1/2} y_P}{\mu} \tag{6}$$

where: C- model constant ; k_P- turbulence kinetic energy at point P; y_P- distance from point P to the wall. In calculations this parameter was in the range between 40 and 80. Boundary conditions in the outlet opening emulate the fully developed flow in duct.

5. Comparison of experimental and numerical data

The velocity field in the horizontal plane located on the level of the air-supply duct is shown in Fig 3. Within the investigated area, two zones with recirculating flow can be distinguished. In the first zone, extended to about 1.0 m from the inlet, there is intensive air mixing. At distances further away from the inlet than 1.0m, the second vortex tends to form. The vorticity magnitudes in these two regions have the opposite sign. In contrast to measurement results and RSM simulations, the calculations relying on the k-ε model reveal a third zone with recirculating flow in the vicinity of the chamber's blind wall.

Fig. 3 (bottom) shows the velocity field contours in the horizontal plane on the level of the axis of inlet opening. To better highlight the characteristic flow features, the coloured velocity scale is restricted to the interval (-1.8 m/s, 2.2 m/s). Velocities beyond that range are represented by extreme colours in the attached colour scale. The inlet is situated near the right upper chamber corner. The air jet entering the system tends to flow towards the left wall of the chamber. Starting from the distance of 1.05m from the inlet, the air jet begins to flow towards the blind wall, along the left-hand side wall of the chamber. The virtual stream of air flowing into system, determined with the use of the k-ε model reaches the left side wall of the chamber approximately 0.8m from the inlet. More accurate values of this parameter,

approaching the accuracy levels available in experiments, were obtained with the use of the RSM model.

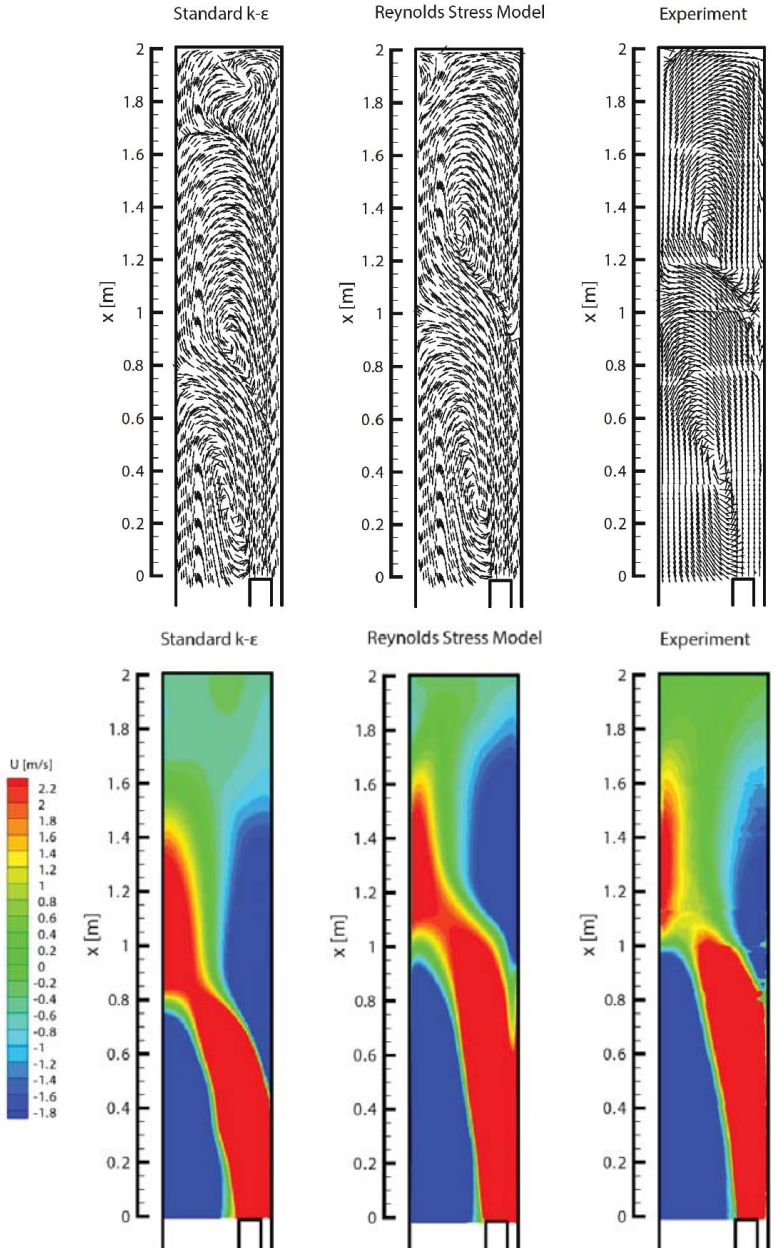

Figure 3. Velocity vectors (top) and velocity magnitude (bottom) in the horizontal plane located on the level of the axis of inlet opening

In the latter case the inlet jet tends to adhere to the left-side wall 1.0m from the inlet. Such a velocity field pattern is obtained both from measurements and simulations using the RMS model and agrees well with the results of investigations conducted in the copper mine chambers.

The experimental and numerical data are compared quantitatively in Fig.4 and Fig.5. These figures show the distributions of two velocity vector components along the selected lines. Horizontal lines are

situated on the level of the axis of the air supply duct and 5 cm above the chamber bottom, the distance from the inlet being 0.5 m, 1.0 m and 1.5 m.

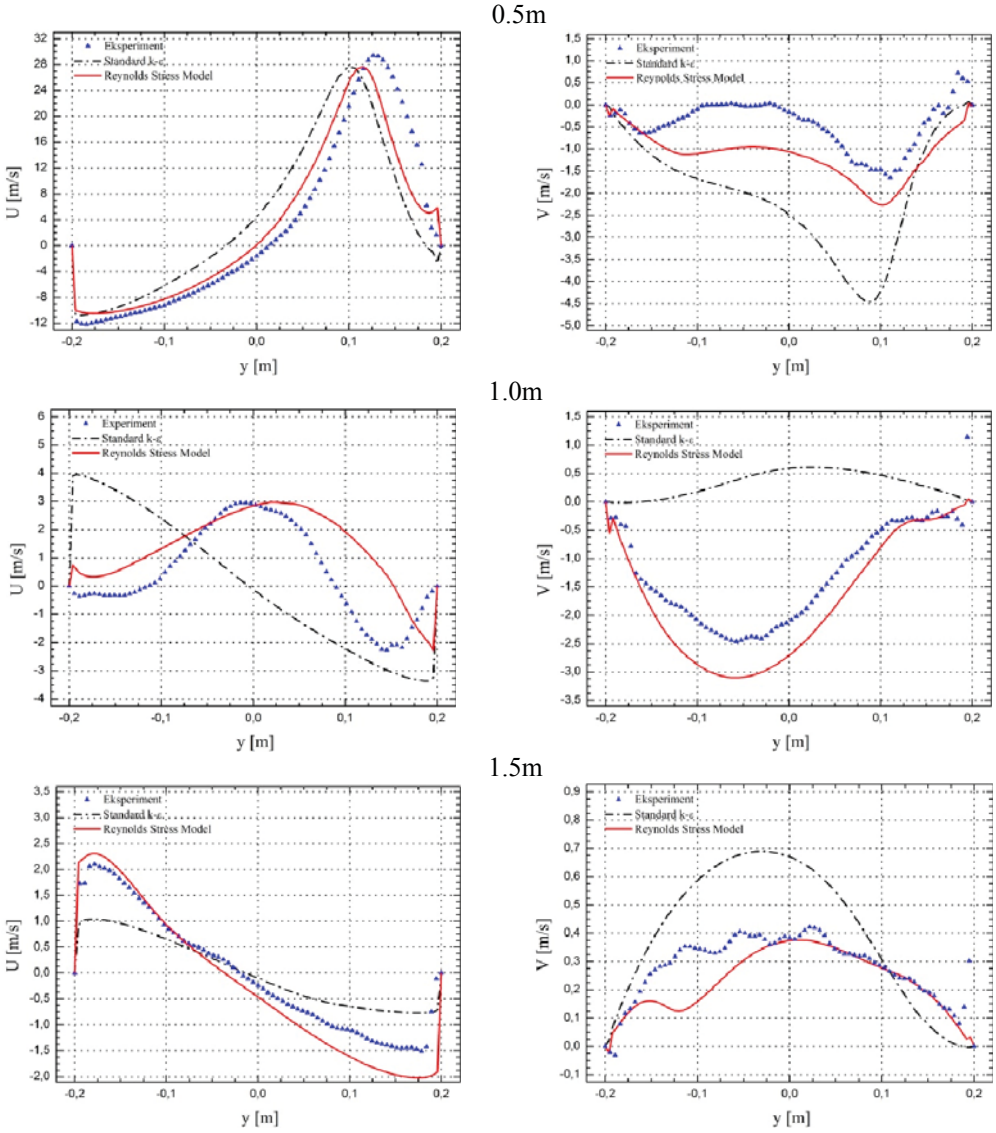

Figure 4. Distribution of the longitudinal *U* and streamwise *V* velocity component along horizontal lines on the level of the axis of inlet opening.

The RSM model provides better predictions than the standard *k-ε* model. In the horizontal cross-section on the level of the axis of supply duct, the longitudinal and streamwise components of the velocity vector obtained using the RSM model agree well with the experimental data (Fig.4). Considerable differences between the experimental and numerical simulation results are registered for the lower chamber regions (Fig.5), particularly for the distance of 1 m from the inlet. These discrepancies are revealed in the region separating two zones with recirculating flow (Fig.3). Despite some discrepancies between the experimental and calculation data, it is still reasonable to conclude

that the RSM model captures the real flows with sufficient accuracy for the needs in ventilation problems.

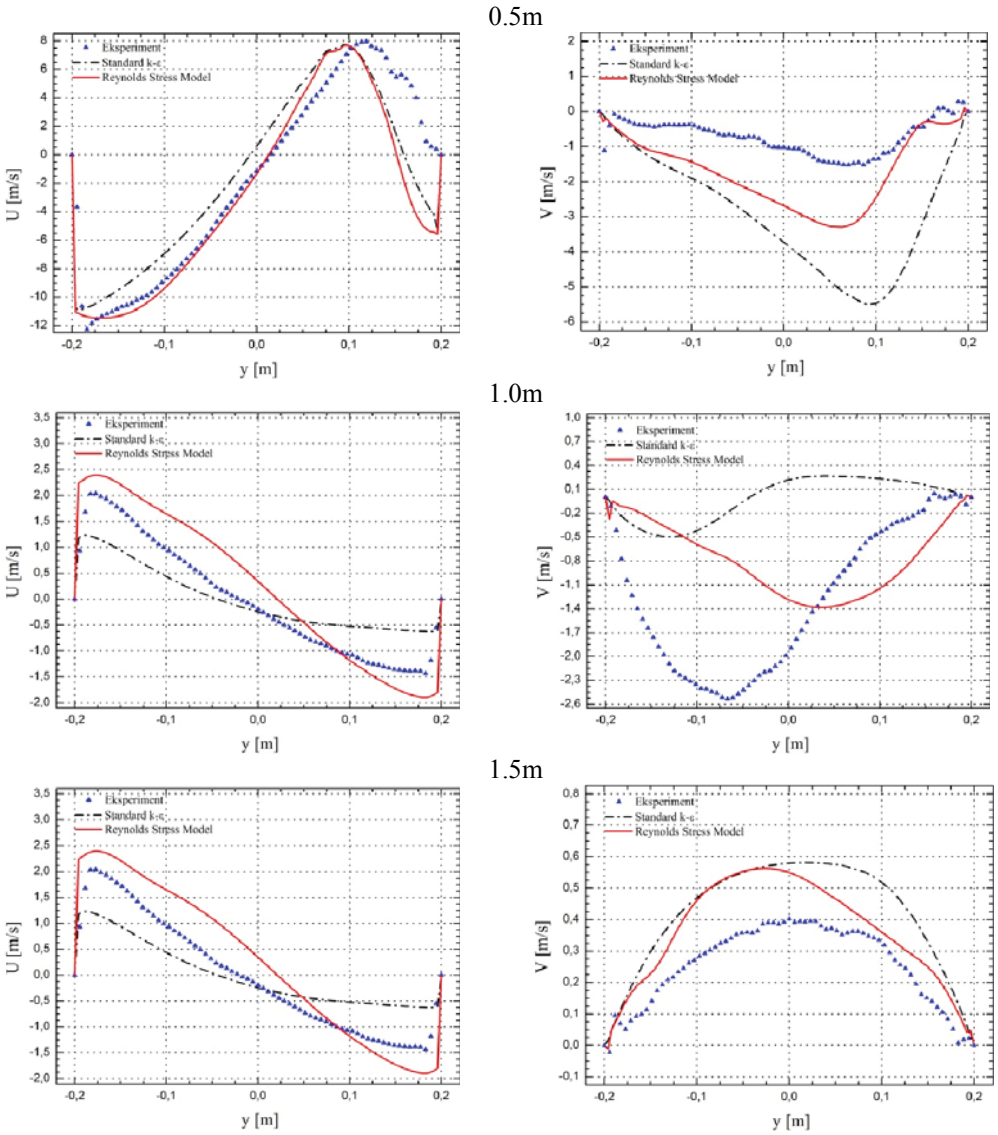

Figure 5. Distribution of the longitudinal *U* and streamwise *V* velocity component along horizontal lines 5 cm above the bottom

6. Conclusion

Two zones with recirculating flow can be distinguished due to the shape of the velocity field created by the inlet air jet. The first zone extends approximately 1m from the inlet. Another vortex rotating in the opposite direction is formed further from the inlet. Such a velocity field pattern is obtained from measurements and qualitative agrees well with numerical data obtained using the RSM model. The RSM model provides better predictions than the standard *k-ε* model. The largest quantitative

differences between the calculated (RSM model) and measured velocity vector components are registered in the lower section of the blind chamber, particularly in the zone separating the recirculating flow regions. Despite these discrepancies, it is reasonable to conclude that computer simulations offer a good insight into ventilation processes in long blind headings aired with jet fans and that the RSM model captures the real flow features with sufficient accuracy for the needs of mine ventilation practices.

Acknowledgements
The research was supported by the Polish Ministry of Science and Higher Education (project No. 4653/B/T02/2010/39)

7. References

[1] Aminossadati, S.M., Hooman K.,2008: Numerical simulation of ventilation air flow in underground mine workings. 12th U.S./North American Mine Ventilation Symposium, 253-259
[2] Krawczyk J., 2007: Single and multiple-dimensional models of unsteady air and gas flows in underground mines (in polish), Archives of Mining Sciences, Monograph, 2
[3] Kuan, B., Yang, W., Schwarz, M.P., 2007: Dilute gas-solid two-phase flows in a curved 90° duct bend: CFD simulation with experimental validation. Chemical Engineering Science, 62, 2068-2088
[4] Nakayama, H., Hirota, M., Shinoda, K., Koide, S., 2005: Flow Characteristics in a Counter-Flow Type T-junction. Thermal Science and Engineering, 13, 17-2
[5] Mossad R., Yang W., Schwarrz M.P., 2009:Numerical prediction of air flow in a sharp 900 elbow, Seventh International Conference on CFD in the Minerals and Process Industries, CSIRO, Melbourne,Australia, 1-5
[6] Rodi,W., 1979: Turbulence Models and their Application in Hydraulics. Delft: IAHR
[7] Skotniczny P., 2013: Three Dimensional Numerical Simulation of Mass Exchange Between Longwall Headings and Goafs, in the Presence of Methane Drainage in U-Type Ventilated Lonwall, Archives of Mining Sciences, 58, 3
[8] Szmyd J., Branny M., Karch M., Wodziak W., Jaszczur M., Nowak R., 2013: Experimental and numerical analysis of the air flow in T-shape channel flow, Archives of Mining Sciences, 58,2, 333–348
[9] Wala A.M., Vytla S., Taylor C.D., Huang G., 2007: Mine face ventilation: a comparison of CFD results against benchmark experiments for CFD code validation, Mining Engineering, 59, 10-17
[10] Wala, A.M., Vytla, A., Huang G. & Taylor C.D. 2008: Study on the effects of scrubber operation on the face ventilation. 12th U.S. North American Mine Ventilation Symposium 2008 Reno, USA